Oxidized In-containing III-V(100) surfaces: Formation of crystalline oxide films and semiconductor-oxide interfaces

M. P. J. Punkkinen,[1,2,*] P. Laukkanen,[1,3,†] J. Lång,[1] M. Kuzmin,[1,4] M. Tuominen,[1] V. Tuominen,[1] J. Dahl,[1] M. Pessa,[3] M. Guina,[3] K. Kokko,[1] J. Sadowski,[5] B. Johansson,[2,6] I. J. Väyrynen,[1] and L. Vitos[2,6,7]

[1]*Department of Physics and Astronomy, University of Turku, FI-20014 Turku, Finland*

[2]*Applied Materials Physics, Department of Materials Science and Engineering, Royal Institute of Technology, SE-10044 Stockholm, Sweden*

[3]*Optoelectronics Research Centre, Tampere University of Technology, FI-33101 Tampere, Finland*

[4]*Ioffe Physical-Technical Institute of the Russian Academy of Sciences, St. Petersburg 194021, Russian Federation*

[5]*MAX-lab, Lund University, SE-221 00 Lund, Sweden*

[6]*Condensed Matter Theory Group, Physics Department, Uppsala University, SE-75121 Uppsala, Sweden*

[7]*Research Institute for Solid State Physics and Optics, P.O. Box 49, H-1525 Budapest, Hungary*

(Received 26 April 2011; published 31 May 2011)

Previously found oxidized III-V semiconductor surfaces have been generally structurally disordered and useless for applications. We disclose a family of well-ordered oxidized InAs, InGaAs, InP, and InSb surfaces found by experiments. The found epitaxial oxide-III-V interface is insulating and free of defects related to the harmful Fermi-level pinning, which opens up new possibilities to develop long-sought III-V metal-oxide-semiconductor transistors. Calculations reveal that the early stages in the oxidation process include only O-III bonds due to the geometry of the III-V(100)$c(8 \times 2)$ substrate, which is responsible for the formation of the ordered interface. The found surfaces provide a different platform to study the oxidation and properties of oxides, e.g., the origins of the photoemission shifts and electronic structures, using surface science methods.

DOI: 10.1103/PhysRevB.83.195329 PACS number(s): 81.10.St, 68.37.−d, 68.43.Bc, 73.61.−r

I. INTRODUCTION

Knowledge of the properties of oxidized semiconductor surfaces is important not only for understanding fundamental issues of material oxidation[1] but also for developing various applications. The mainstream of current transistor technology, silicon-based metal-oxide-semiconductor-field-effect transistors (MOSFETs), is facing its fundamental limits as manufacturers are continuously striving for better performance and higher packing density in their products. Therefore, new alternatives for channel and gate-insulator materials have been under intensive research.[2–7] III-V compound semiconductors such as InAs, InGaAs, InGaSb, and InP would be ideal channel materials for future MOSFETs due to their superior electron mobilities compared to Si. Significant efforts have been initiated at both university and industry laboratories to produce gate-insulator interfaces of III-V channel layers that are stable and meet commercial-device criteria as successfully as the SiO_2-Si junction does. However, despite intense research, this great goal, which would lead to significantly increased lifetime and performance of devices and energy savings at data servers, has not yet been achieved.

Oxidation of the III-V compound semiconductors is also of considerable relevance in other technological contexts such as semiconductor protection, electrical insulation devices, antireflection coatings of solar cells, and metal contacts for semiconductor devices. However, there is much room to improve our understanding of oxidized III-V surfaces and semiconductor oxidation in general; even the SiO_2-Si system is still intensively investigated.[8–10] The amorphous state of oxidized semiconductor surfaces has hindered investigations of these surfaces because it has been difficult to utilize the standard surface science tools[11] such as scanning tunneling microscopy (STM) and diffraction, as well as valence-band dispersion probes, in the studies of oxidized semiconductors without long-range order. This is in drastic contrast to well-defined surface oxides of many metals[12–18] that are important for the applications of catalysis. To our best knowledge, a crystalline oxide surface has been found only for GaN,[19] but GaN does not crystallize in the zincblende structure, as do most of the III-V's, and does not have carrier mobilities suitable for future MOSFETs. Schäfer *et al.* have reported epitaxial In_2O_3 islands on InAs.[20] Previous core-level photoemission measurements of amorphous III-V surface oxides, combined with phase diagrams, have provided important information about different oxygen-containing compounds formed and various oxidation states for the group-III and -V elements.[5,21] However, the knowledge of atomic and electronic structures of oxidized III-V surfaces, which is essential to understand the oxidation processes and to employ these surfaces in a controlled way in device development, is far from complete.

Therefore, our findings of long-range ordered oxides on several III-V surfaces are of significant fundamental and practical interest. The presence of amorphous III-V surface oxides, which cause the Fermi-level pinning via the high density of defect states at the semiconductor-insulator interface, is detrimental to transistors. Therefore, a huge amount of work has been undertaken to understand how III-V oxides can be removed (or their formation prevented) during the manufacturing of insulator-III-V junctions. It is still unclear whether it is possible to avoid the oxygen reaction during interface growth. There are different models that explain the Fermi-level pinning. It is important to note that irrespective of the specific oxides, vacancies, metallic clusters, antisites, or broken two-dimensional periodicity called for to explain the Fermi-level pinning,[5,22] there should be much less harmful defects in a crystalline epitaxial semiconductor-insulator interface. The connection between the disordered interface and the interface states has been shown.[23] It has been also

 ©2011 American Physical Society

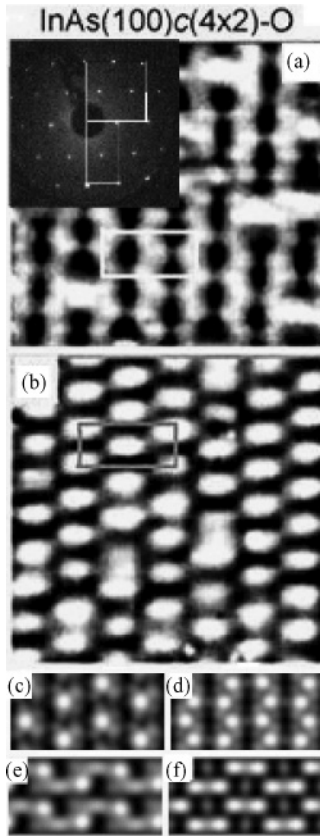

FIG. 1. (a) Measured filled-state (2.54 V) STM image of InAs(100)$c(4 \times 2)$-O. The inset shows LEED (32 eV) from InAs(100)$c(4 \times 2)$-O; white square shows the (1×1) unit cell of the substrate plane and white rectangle shows the $c(4 \times 2)$-O unit cell. (b) Measured empty-state (2.40 V) STM image of InAs(100)$c(4 \times 2)$-O. (c) Calculated filled-state (2.54 V) STM image, stable structure. (d) Calculated filled-state (2.54 V) STM image, metastable structure. (e) Calculated empty-state (2.40 V) image, stable structure. (f) Calculated empty-state (2.40 V) image, metastable structure.

found that in a crystalline interface between the metal-oxide film and III-V surface, no pinning occurs.[24,25]

Our low-energy-electron-diffraction (LEED), scanning-tunneling-microscopy (STM), and photoemission measurements (Figs. 1–4) reveal the formation of the InAs(100)$c(4 \times 2)$-O, InAs(100)(3×1)-O, InP(100)(2×3)-O, In/GaAs(100)(4×3)-O, In/GaAs(100)$c(4 \times 2)$-O, InSb(100)(1×2)-O, and InSb(100)(3×1)-O reconstructed layers (the three latter ones are not shown). These well-defined oxidized III-V surface layers provide a crystalline, stable, and defect-free interface enabling a different approach to search for suitable insulator-III-V junctions for long-sought III-V MOSFETs. Very recently, an interesting improvement has been found in a MOSFET test with a thermally grown interfacial $InAsO_x$ layer.[7] This finding supports the applicability of the ordered oxides we found as a "part" of a MOSFET, which is sketched in Fig. 2(g). On the other hand, our finding might provide an explanation for the recent MOSFET improvement. Thus, amorphous or crystalline insulator layers grown on the epitaxial oxide layer, as found here, may provide the junction with increased quality. Our

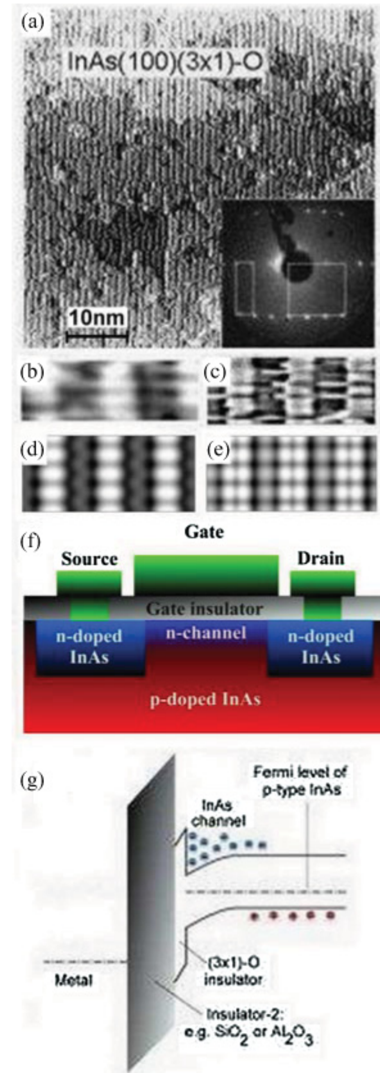

FIG. 2. (Color online) (a) Measured filled-state (2.24 V) STM image of InAs(100)(3×1)-O after air exposure and heating. The inset shows LEED (57 eV) from InAs(100)(3×1)-O; white square shows the (1×1) unit cell and white rectangle shows the unit cell of (3×1)-O. (b) Measured empty-state (0.98 V) STM image of InAs(100) (3×1)-O. (c) Measured filled-state (2.04 V) STM image of InAs(100)(3×1)-O. (d) and (e) Calculated STM images. (f) Scheme for MOSFET. (g) Scheme for utilizing the (3×1)-O layer in MOSFET. A second oxide is grown on top of the (3×1)-O.

findings also show that the same useful thermal oxidation[7] is feasible not only for InAs but more generally for In-containing III-V surface layers.

II. EXPERIMENT

Below we describe the experimental procedure used to obtain ordered oxide films on several III-V surfaces. The III-V surfaces were cleaned by Ar ion sputtering and vacuum annealing, resulting in the $c(8 \times 2)$ reconstruction on GaAs(100), InAs(100), and InSb(100), and the (2×4) reconstruction on InP(100). Two different ordered atomic structures have been proposed for the $c(8 \times 2)$ surface: ζ ("zeta") and ζa ("zeta a")

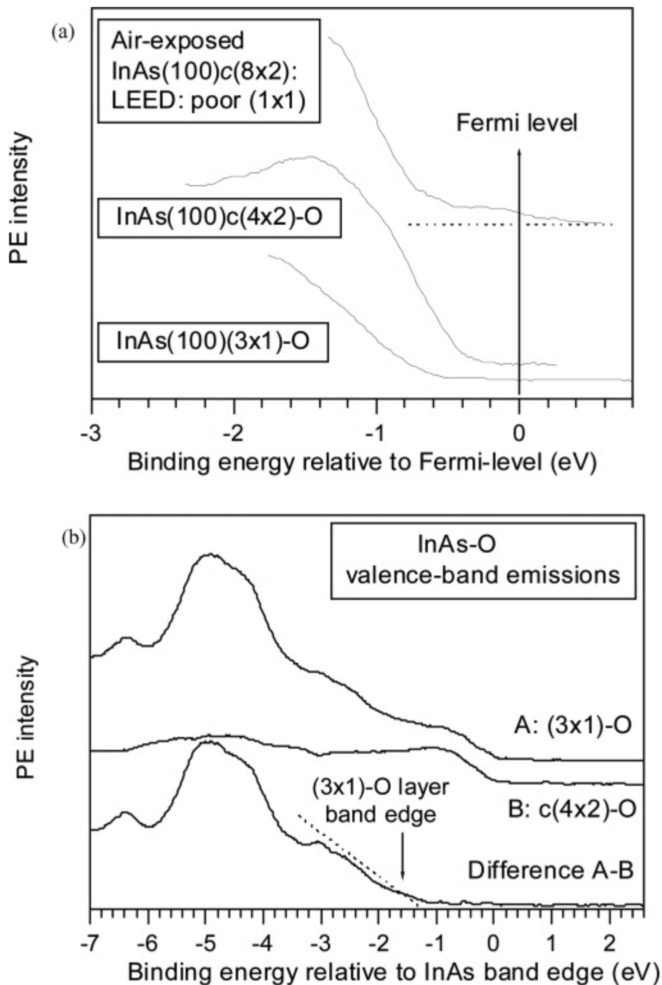

FIG. 3. (a) Photoemission from the InAs(100)(3×1)-O and $c(4 \times 2)$-O layers as well as from an amorphous oxidized InAs surface. (b) Difference spectrum between the (3×1)-O and $c(4 \times 2)$-O. The Fermi level is at 0.4 eV for both surfaces, as deduced from a Ta plate in connection to the sample.

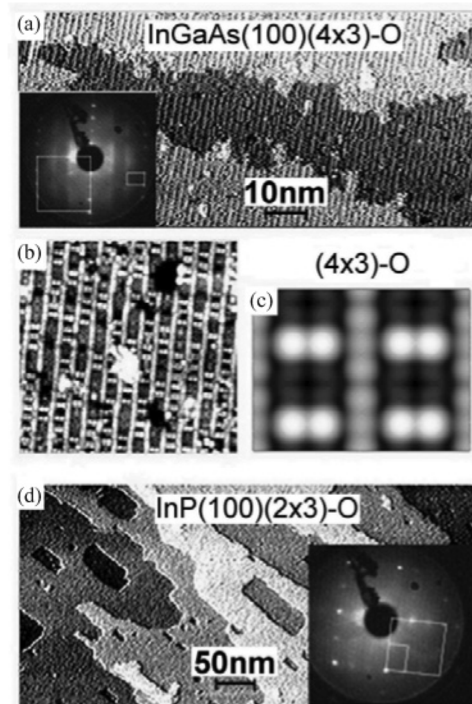

FIG. 4. (a) and (b) Measured filled-state STM images of InGaAs(100)(4×3)-O; -2.54 V and -2.19 V, respectively. The inset of (a) shows LEED from InGaAs(100)(4×3)-O. (c) Calculated filled-state image (-2.19 V) for InGaAs(100)(4×3)-O. (d) Measured empty-state (2.63 V) STM image of InP(100)(2×3)-O surface. The inset shows LEED from InP(100)(2×3)-O.

structures. Figure 5(a) shows the ζa model of In/GaAs. The peculiar feature of this reconstruction is that the first layer is equicomposed of anions and cations. The InGaAs(100)$c(8 \times 2)$ surface was obtained by depositing 1–2 monolayers (ML) of indium on the clean GaAs and heating the sample up to 500–550 °C.[26] The O_2 gas was introduced into a vacuum chamber and the O_2 pressure was $3-4 \times 10^{-6}$ mbar during the oxidation. The O_2 exposure time varied between 5 and 30 min, and the substrate temperature was 350–520 °C, depending on the material (the lowest temperature for InAs and InSb and the highest temperature for InGaAs). These conditions produced smooth topography with two-dimensional islands (Figs. 2 and 4), which is also characteristic for the clean starting substrates.

III. THEORETICAL METHODS

Calculations were performed using an *ab initio* density-functional total-energy method within the local-density approximation.[27,28] The approach is based on the plane-wave basis and projector augmented wave method[29,30] (Vienna *ab initio* simulation package, VASP).[31–34] The optimization of the atomic structure was performed using the conjugate gradient minimization of the total energy with respect to the atomic coordinates. The III-V(100) surfaces were simulated using slabs of 13 or 14 atomic layers, separated by a vacuum 23 Å wide. The $c(8 \times 2)$ reconstruction was modeled by a (4×2) surface unit cell, because the effect of double periodicity on the total energy was found to be very small.[26] The dangling bonds of the bottom surface As atoms were passivated by fractionally charged pseudohydrogen atoms ($Z = 0.75$) and two bottom layers of the slabs were fixed to ideal bulk positions. Other atoms, including pseudohydrogens, were relaxed until the remaining forces were less than 20 meV/Å. The number of k points in the Brillouin zone corresponded to 64 k points in the Brillouin zone of the (1×1) slab. The k-point sampling was performed using the Monkhorst-Pack scheme[35] with the origin shifted to the Γ point. The plane-wave cutoff energy was 400 eV. Theoretical lattice constants of 5.63 and 6.06 Å were obtained and used for GaAs and InAs, respectively. The constant-current STM images were simulated within the Tersoff-Hamann approximation.[36]

IV. RESULTS AND DISCUSSION

First, we consider the ordered oxygen-induced reconstructions on InAs, which also seem to be the most typical ones on the III-V surfaces. A good long-range order for the InAs(100)$c(4 \times 2)$-O surface (heated at 400 °C during the O_2 exposure) is revealed by LEED [inset of Fig. 1(a)] and by STM [Figs. 1(a) and 1(b)]. On the basis of the

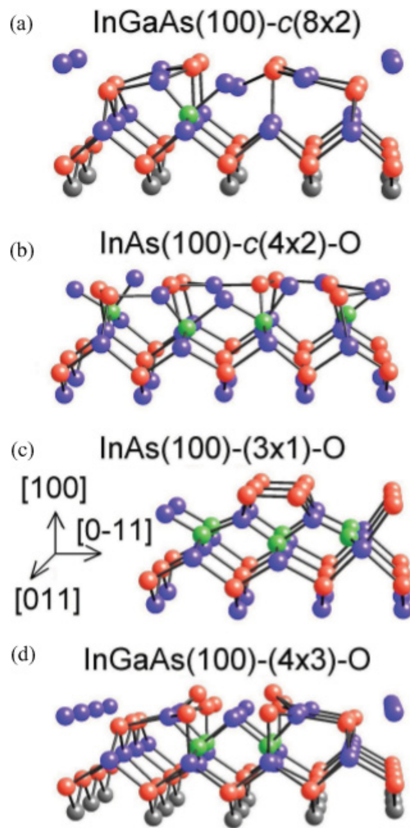

FIG. 5. (Color online) (a) ζa structure of InGaAs(100) surface [(4 × 2) unit cell] with an oxygen atom in a remarkably stable adsorption position (2 MLs of In). (b) Most stable $c(8 \times 2)$ model found (InAs; 0.5 MLs of O). (c) Model candidate for (3 × 1) InAs structure (1 ML of O). (d) InGaAs(100)(4 × 3)-O structure (0.33 MLs of O). The O, In, Ga, and As atoms are shown by green, blue, gray, and red atoms, respectively.

O1s x-ray photoemission intensity analysis (not shown), the oxygen amount in the (3 × 1)-O is twice as high as that of the $c(4\times2)$-O. It is important for applications that the interface is stable. The InAs(100)(3 × 1)-O surface was taken from the vacuum chamber to air for 0.5−1 hours. Then, the surface was loaded back into the vacuum and characterized by the LEED and the STM as a function of the post-heating time. After a one-hour air exposure, the (3 × 1)-O sample exhibited, without any post-heating, a (3 × 1) pattern. Naturally, the pattern became weaker due to the air exposure, but the clear (3 × 1), similar to that in the inset of Fig. 2(a), was recovered after heating at 400 °C. This is supported by the STM image [Fig. 2(a)] from the (3 × 1)-O surface after a 0.5-hour air exposure and post heating at 400 °C. The same air exposure and heating of the clean InAs(100)$c(8 \times 2)$ surface led to a poor (1 × 1) LEED without any clear superstructure, which also demonstrates that it is important to have proper oxidation temperature and pressure to get ordered oxides. Thus, the (3 × 1)-O layer is stable against rather strong air and temperature loadings. It is worth noting that the atomic layer deposition (ALD) of the gate insulators on InAs(100) and InGaAs(100) is usually performed at 250–350 °C substrate temperatures, at which the (3 × 1)-O was clearly stable in our experiments.

The electronic structure of an insulator-semiconductor interface plays a significant role in the MOSFETs. The electronic structures of the InAs(100)$c(4 \times 2)$-O and InAs(100)(3 × 1)-O layers were characterized by synchrotron radiation photoelectron spectroscopy (MAX-lab, Sweden) and scanning tunneling spectroscopy (STS). The photoemission results in Fig. 3(a) show a semiconducting system without electron states around the Fermi level, which is a clear sign of the absence of the Fermi-level pinning. It is important to note that band bending, which is sensitive to defects, did not occur as compared to the clean InAs(100)$c(8 \times 2)$. This is concluded from the bulk In 3d and As 3d core-level binding energies, which are not changed within ±0.1 eV according to a preliminary analysis, as the oxide layer is formed. Also scanning tunneling spectroscopy (STS) shows that the oxide phases do not cause defect states in the InAs band gap. The valence-band maximum difference between the InAs substrate and (3 × 1)-O layer is estimated in Fig. 3(b) using a difference spectrum between the InAs(100)(3 × 1)-O and InAs(100)$c(4 \times 2)$-O spectra, in which the InAs band edge is basically removed. This gives an estimation for the (3 × 1)-O valence-band edge: it is at a binding energy that is 1.0–1.4 eV higher than the InAs one. STS shows a movement of the surface conduction-band edge toward the vacuum in the oxide phase compared to the InAs edge.

The detailed chemistry and geometry of the investigated surfaces were determined by total-energy optimization. Since in the experiments the initial adsorption of oxygen is on the $c(8 \times 2)$ surface, the optimization procedure was started by determining the energetically most favorable position of one oxygen atom on this surface. Figure 5(a) shows the In/GaAs surface with an O atom in its energetically most favorable site. The stability of this one-atom adsorption site, which locates in the second surface layer, i.e., below the surface, is quite distinct (∼1 eV more stable than the other sites). This is in remarkable contrast, e.g., to the common $\beta(2 \times 4)$ surface, which was also considered. The exceptional stability of this adsorption site can be related to the binding of the electronegative O atom to four electropositive In atoms. It is important to note that this kind of adsorption site is found because the peculiar $c(8 \times 2)$ structure includes a mixed (III-V) first surface layer.

An ordered oxidized surface with the lowest O coverage (less than 0.5 ML) was found only on the In/GaAs(100)(4 × 3)-O surface. The formation of this reconstruction is easily understood. The stable, equivalent one-atom adsorption positions [four per (4 × 2) cell] that were found are gradually filled. Because the O atoms cause strain in the lattice (especially in the [011] direction), it is energetically favorable for the surface to keep periodically empty adsorption positions in the [011] direction. Figure 4(c) shows the simulated STM image of the In/GaAs(100)(4 × 3)-O surface shown in Fig. 5(d), which is in good agreement with the corresponding experimental image in Fig. 4(b).

InAs(100)$c(4 \times 2)$-O reconstruction is found around 0.5 ML. Inspired by the pronounced stability of the adsorption position in the second layer, a quite symmetric atomic model was designed based on the original $c(8 \times 2)$-ζa reconstruction. Figure 5(b) shows the resulting most stable model, while a slightly more symmetric metastable structure was also found. The simulated STM images for the metastable structure

[Figs. 1(d) and 1(f)] agree well with the experimental images in Figs. 1(a) and 1(b). This kind of image could also be due to periodic atomic movements within the stable structure, in a similar way as happens on the pure Si(100)$p(2 \times 2)$ surface.[37]

When the oxygen coverage is increased over 0.5 ML, two things happen. First, all In atoms move below the first layer. The O atoms are sandwiched between successive In atom layers, which makes the structure quite stable. Second, the $\times 4$ periodicity is changed to the $\times 3$ periodicity, which is caused by the increased strain due to the increased amount of O. Figure 5(c) shows one of the atomic model candidates for the O/InAs(100)(3×1) surface with 1 ML of O. We note that for all reconstructions, we were able to find structures having an energy gap. However, deductions concerning the energy-gap size are not possible due to the well-known shortcomings of the local-density approximation (LDA) when applied to oxides. Overall, calculations reveal that the general geometrical features of the found structures can be described in a good agreement with experiments. It is important to note that the current models for the (3×1) layer have the zincblende structure if the As atoms on top of the surface are neglected, i.e., the oxide interface is epitaxial, which provides an opportunity to grow another insulator layer epitaxially on the (3×1) layer. In the future, it will be interesting to test for an example of the growth of BaO layers on the found crystalline oxidized surfaces.

Similarly ordered oxidized superstructures were not found on the GaAs(100), although the LEED pattern suggested (3×1) periodicity on the GaAs after its oxidation at elevated temperatures (around 650 °C). This treatment made the surface rough. The nonexistence of the ordered oxide on the GaAs could be explained by the oxygen-induced strain, which is large on the GaAs due to the small lattice parameter. On the other hand, reconstruction change from the ζ reconstruction to the ζa reconstruction was found as the cation size in the surface layer was increased at 0 K.[26] The additional cations in the first layer on cell edges of the ζa structure (compared to the ζ reconstruction) are needed to allow the formation of the oxides explained above, and therefore the reconstruction change may explain the appearance of the ordered oxide on the GaAs at elevated temperatures. Ohtake *et al.* found evidence for the stability of the ζa type reconstruction on the GaAs(100) surface above 600 °C.[38]

V. CONCLUSIONS

We have shown that there exist crystalline oxidized III-V surface layers having a zincblende parent structure. It can now be understood why these layers may not have been found previously: these oxidized surface layers arise from a complex interplay of the proper starting surface, substrate temperature, and oxygen pressure. Our extraordinary findings are attributed to the peculiar starting $c(8 \times 2)$-ζa surface, which enables the formation of stable adsorption sites with only nearest-neighbor indium atoms, and results in ordered oxide. Our findings open up new possibilities to design interfaces for MOSFETs, and may provide an explanation for the recent results in which an oxidized InAs layer was used. We anticipate that our results are useful also for general studies of the oxidation on semiconductor surfaces.

ACKNOWLEDGMENTS

We are grateful to H. Ollila and the MAX-lab staff for technical assistance. The calculations were performed using the facilities of the Finnish IT Center for Science (CSC) and the Mgrid project (Turku, Finland). This work has been supported by the Academy of Finland Grants No. 122743 and No. 122355, as well as Finnish Academy of Sciences and Letters. The Swedish Research Council, the Swedish Foundation for Strategic Research, the Swedish Energy Agency, the National Graduate School in Materials Physics, Solar III-V project (Dnro: 3120/31/08), the Carl Trygger Foundation, the Turku University Foundation, the Emil Aaltonen Foundation, and the Göran Gustafsson Foundation are also acknowledged for financial support.

---

*Author to whom correspondence should be addressed. marko.punkkinen@utu.fi
†pekka.laukkanen@utu.fi
[1] *Fundamental Aspects of Silicon Oxidation*, edited by Y. J. Chabal (Springer, New York, 2001).
[2] C. W. Wilmsen and S. Szpak, Thin Solid Films **46**, 17 (1977), and references therein.
[3] W. F. Crydon and E. H. C. Parker, *Dielectric Films on Gallium Arsenide* (Gordon and Breach, New York, 1981).
[4] *Physics and Chemistry of III-V Compound Semiconductor Interfaces*, edited by C. W. Wilmsen (Plenum, New York, 1985).
[5] *Fundamentals of III-V Semiconductor MOSFETs*, edited by S. Oktyabrsky and P. D. Ye (Springer, New York, 2010).
[6] P. D. Ye, Compd. Semicon. **14**, 29 (2008).
[7] H. Ko, K. Takei, R. Kapadia, S. Chuang, H. Fang, P. W. Leu, K. Ganapathi, E. Plis, H. S. Kim, S.-Y. Chen, M. Madsen, A. C. Ford, Y.-L. Chueh, S. Krishna, S. Salahuddin, and A. Javey, Nature (London) **468**, 286 (2010).
[8] A. Pasquarello, M. S. Hybertsen, and R. Car, Nature (London) **396**, 58 (1998).
[9] A. Hemeryck, A. Estève, N. Richard, M. Djafari Rouhani, and Y. J. Chabal, Phys. Rev. B **79**, 035317 (2009).
[10] B. Gokce, E. J. Adles, D. E. Aspnes, and K. Gundogdu, Proc. Natl. Acad. Sci. USA **107**, 17503 (2010).
[11] C. B. Duke, Proc. Natl. Acad. Sci. USA **100**, 3858 (2003).
[12] H. Over, Y. D. Kim, A. P. Seitsonen, S. Wendt, E. Lundgren, M. Schmid, P. Varga, A. Morgante, and G. Ertl, Science **287**, 1474 (2000).
[13] C. I. Carlisle, D. A. King, M.-L. Bocquet, J. Cerdá, and P. Sautet, Phys. Rev. Lett. **84**, 3899 (2000).
[14] M. Todorova, W. X. Li, M. V. Ganduglia-Pirovano, C. Stampfl, K. Reuter, and M. Scheffler, Phys. Rev. Lett. **89**, 096103 (2002).
[15] V. Maurice, G. Despert, S. Zanna, M.-P. Bacos, and P. Marcus, Nature Mater. **3**, 687 (2004).
[16] A. Stierle, F. Renner, R. Streitel, H. Dosch, W. Drube, and B. C. Cowie, Science **303**, 1652 (2004).

[17] J. Schnadt, A. Michaelides, J. Knudsen, R. T. Vang, K. Reuter, E. Lægsgaard, M. Scheffler, and F. Besenbacher, Phys. Rev. Lett. **96**, 146101 (2006).
[18] M. Schmid, A. Reicho, A. Stierle, I. Costina, J. Klikovits, P. Kostelnik, O. Doubay, G. Kresse, J. Gustafson, E. Lundgren, J. N. Andersen, H. Dosch, and P. Varga, Phys. Rev. Lett. **96**, 146102 (2006).
[19] Y. Dong, R. M. Feenstra, and J. E. Northrup, J. Vac. Sci. Technol. B **24**, 2080 (2006).
[20] M. Schäfer, W. Naumann, T. Finnberg, M. Hannss, A. Dutschke, and R. Anton, Appl. Surf. Sci. **158**, 147 (2000).
[21] G. Hollinger, R. Skheyta-Kabbani, and M. Gendry, Phys. Rev. B **49**, 11159 (1994).
[22] H. Hasegawa, Jpn. J. Appl. Phys. **38**, 1098 (1999).
[23] H. Hasegawa, L. He, H. Ohno, T. Sawada, T. Haga, Y. Abe, and H. Takahashi, J. Vac. Sci. Technol. B **5**, 1097 (1987).
[24] M. Hong, J. Kwo, A. R. Kortan, J. P. Mannaerts, and A. M. Sergent, Science **283**, 1897 (1999).
[25] M. J. Hale, S. I. Yi, J. Z. Sexton, A. C. Kummel, and M. Passlack, J. Chem. Phys. **119**, 6719 (2003).
[26] J. J. K. Lång, M. P. J. Punkkinen, P. Laukkanen, M. Kuzmin, V. Tuominen, M. Pessa, M. Guina, I. J. Väyrynen, K. Kokko, B. Johansson, and L. Vitos, Phys. Rev. B **81**, 245305 (2010).
[27] D. M. Ceperley and B. J. Alder, Phys. Rev. Lett. **45**, 566 (1980).
[28] J. P. Perdew and A. Zunger, Phys. Rev. B **23**, 5048 (1981).
[29] P. E. Blöchl, Phys. Rev. B **50**, 17953 (1994).
[30] G. Kresse and D. Joubert, Phys. Rev. B **59**, 1758 (1999).
[31] G. Kresse and J. Hafner, Phys. Rev. B **47**, 558 (1993).
[32] G. Kresse and J. Hafner, Phys. Rev. B **49**, 14251 (1994).
[33] G. Kresse and J. Furthmüller, Comput. Mat. Sci. **6**, 15 (1996).
[34] G. Kresse and J. Furthmüller, Phys. Rev. B **54**, 11169 (1996).
[35] H. J. Monkhorst and J. D. Pack, Phys. Rev. B **13**, 5188 (1976).
[36] J. Tersoff and D. R. Hamann, Phys. Rev. Lett. **50**, 1998 (1983); Phys. Rev. B **31**, 805 (1985).
[37] R. A. Wolkow, Phys. Rev. Lett. **68**, 2636 (1992).
[38] A. Ohtake, S. Tsukamoto, M. Pristovsek, N. Koguchi, and M. Ozeki, Phys. Rev. B **65**, 233311 (2002).